

Comparative Study of Morphology and Optical Properties of SrAl_4O_7 Nano- Phosphors

V. T. Jisha

Research Centre, S.T. Hindu College, Nagercoil -629 002, Tamilnadu, India

Abstract: *Strontium aluminate nanophosphor SrAl_4O_7 was prepared by sol-gel method. The obtained materials were characterized by SEM, XRD, EDAX and PL. Monoclinic structure was confirmed by X-ray diffraction analysis, particle size was determined by Scherrer formula. The particles were of somewhat round shaped and interlinked with each other, leading to the formation of bigger particles. Also some irregular aggregations were found in the image. Photoluminescence emission was at 395, 520 and 790 nm corresponding to UV, green and IR regions under excitation at 360 nm.*

Keywords: XRD, FTIR, SEM, sol-gel method, Photoluminescence

1. Introduction

Alkaline earth metal oxides combined with aluminium oxide are of great interest in material science because of use as long duration photoluminescence and thermoluminescence pigments. They have potential use as refractory oxides in the steel industry and binder materials in the cement industry [1]. Many efforts have been made to discover host materials as well as activators with high performance for phosphor applications. Sol-gel method represents an attractive and easy alternative method to conventional synthesis method, such as ceramic firing [2-4], precipitation [5, 6], or ion exchange on supported oxides [7]. The sol-gel process is an efficient technique for the preparation of phosphors due to the good mixing of starting materials and relatively low reaction temperature resulting in more homogeneous products than those obtained by direct solid state reactions. With sol-gel technique, a low temperature (950°C) has been reported for the successful preparation of MgAl_2O_4 powders [8]. In this work, preparation of SrAl_4O_7 :La, structure, morphology and luminescence were reported. In recent years, rare earth (RE) doped nanomaterials have attracted wide use in various applications as thin film electroluminescent (TFEL) devices, optoelectronic or cathodoluminescent devices. RE-doped insulators are used in telecommunications, lasers and amplifiers, medical analysis and phosphors, etc. Generally rare earth doped aluminates have greater impact on defect centers within the band gap. The emission of light from the ultra violet, visible and Infra red depends on the host material properties [14-18].

2. Experimental

The Sol-gel procedure of synthesizing nanoparticles is thoroughly described as follows: 98wt% of 2M Strontium

acetate $[(\text{CH}_3\text{COO})_2\text{Sr} \cdot 2\text{H}_2\text{O}]$ was dissolved in 25 ml of 2-methoxyethanol with vigorous stirring. All starting materials used in the experiments were in analytical grade and of the high purity. Simultaneously, 5 wt. % of 2M Aluminum acetate $[\text{C}_4\text{H}_6\text{AlO}_4 \cdot 4\text{H}_2\text{O}]$ was dissolved in 25 ml of 2-methoxyethanol with vigorous stirring and subsequently, it was added to the first solution to reach 50 ml in total. Then it was stirred for 30 min at room temperature for the second time. Ammonia was slowly added to this solution with a constant stirring until a pH of 10.5 was achieved. After the stirring of the solution for 30 min, acetic acid and ethylene glycol in the ratio 1:1 was added to the solution. The sol was heated at 80°C while being mechanically stirred with a magnetic stirrer. As the evaporation proceeded, the sol turned into a viscous gel. The gel was aged for 2h and then dried at 100°C for about 5h. The resulting materials were well grinded and annealed at 950°C for 5h to obtain SrAl_4O_7 nanopowders. The same procedure was repeated with the 10wt% of Aluminum acetate.

3. Results and Discussion

1. Morphological Study

SEM Analysis

Figure 1 shows the SEM image of SrAl_4O_7 . The micrograph indicates that nearly all the powder particles were composed of same shape nanoparticles. The presence of bigger particles is attributed to the growth of small particles, which is a result of the sol-gel synthesis. Under the reaction time and temperature, some of the tiny particles underwent a self-induced process, aggregate and growth forming bigger particles.

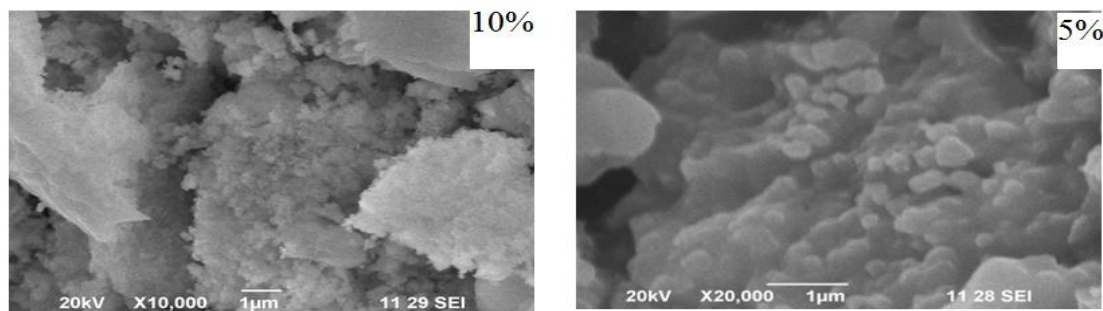


Figure 1: The SEM image of SrAl_4O_7

X-Ray Diffraction (XRD)

The structure and phase purity of the SrAlO phosphor were investigated by XRD. The XRD patterns were obtained and are shown in Fig.2 for SrAlO diffraction patterns were obtained using $\text{CuK}\alpha$ radiation ($\lambda=1.54051 \text{ \AA}$). Measurements were made from $2\theta=10^\circ$ to 80° with steps of 0.02° . The XRD patterns of the powders revealed that the structure of SrAl_4O_7 is Monoclinic, which is match with JCPDS data card No. 25-1289. The crystallites are less than approximately 50-90nm in size appreciable broadening in the X-ray diffraction lines. SEM images SrAl_4O_7 which is un-uniform and may be due to the formation of fractal attribution to sort of self organization. SEM image of SrAl_4O_7 sintered at 900°C for 3hrs appears to irregular

shape. The peaks resolved by X-ray diffraction analysis are observed at $19.79, 22.05, 25.199, 25.928, 27.26, 28.39, 30.604, 31.866, 33.60, 34.82, 36.206, 36.500, 36.604, 39.284, 40.402, 43.23, 44.54, 45.394, 46.104, 47.727, 49.984, 51.570, 53.57, 55.10, 56.167, 58.13, 58.937, 59.89, 61.5, 62.80, 63.96, 65.146, 72.69$ and 73.62 diffraction angle which are assigned to $0\ 2\ 0, 1\ 1\ 1, \bar{3}\ 1\ 1, 0\ 2\ 1, \bar{2}\ 2\ 1, 4\ 0\ 0, 1\ 3\ 0, 2\ 2\ 1, 0\ 0\ 2, \bar{4}\ 2\ 0, 1\ 3\ 1, \bar{5}\ 1\ 1, \bar{3}\ 3\ 0, \bar{3}\ 2\ 2, 2\ 0\ 2, 3\ 3\ 1, \bar{1}\ 3\ 2, 2\ 2\ 2, \bar{3}\ 3\ 2, 1\ 3\ 2, 4\ 4\ 0, 7\ 0\ 0, \bar{2}\ 2\ 3, 1\ 1\ 3, \bar{4}\ 4\ 2, 1\ 2\ 3, 7\ 0\ 1, \bar{2}\ 0\ 2, \bar{2}\ 5\ 2, 7\ 2\ 1, 2\ 6\ 0, \bar{2}\ 6\ 1, \bar{6}\ 0\ 4$ and $\bar{8}\ 4\ 0$. The average particle size of the samples obtained at 5 and 10 wt% are 62 and 90nm respectively. That indicates that the average particle size increases with the increase of the Al concentration.

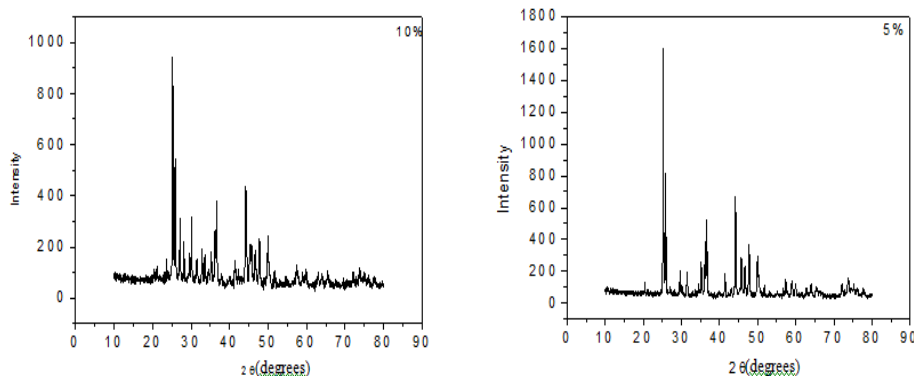


Figure 2: The XRD image of SrAl_4O_7

In order to determine the crystallite size of powder, the Williamson–Hall plot has been used as a useful tool for graphical demonstration of any hkl -dependence of broadening within a particular diffraction pattern. In the Williamson–Hall

method ,it is assumed that the line broadening β_D of a Bragg reflection (hkl) originating from the small crystallite size follows the Scherrer equation $D=K\lambda/\beta\cos\theta_{hkl}$.

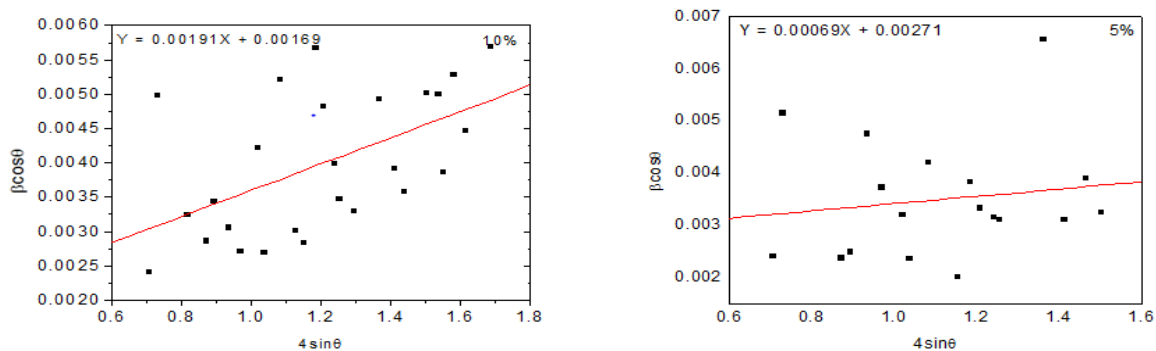


Figure 3: Williamson–Hall plot of SrAl_4O_7

Plotting the value of $\beta_{hkl}\cos\theta_{hkl}$ as a function of $4\sin\theta_{hkl}$, the microstrain ϵ may be estimated from the slope of the line and the crystallite size from the intersection with the vertical

axis. Crystallite size of the particles is measured on average as 51 and 82nm before and after thermal treatment, respectively. The difference between Scherrer and

Williamson–Hall may be due to the effects of internal strain not considered in the Scherrer model.

EDAX Analysis

The chemical composition of the SrAl_4O_7 phosphors can be determined by the energy dispersive X-rays spectroscopy. Fig. 4 shows the energy dispersive spectrum of the SrAl_4O_7 .

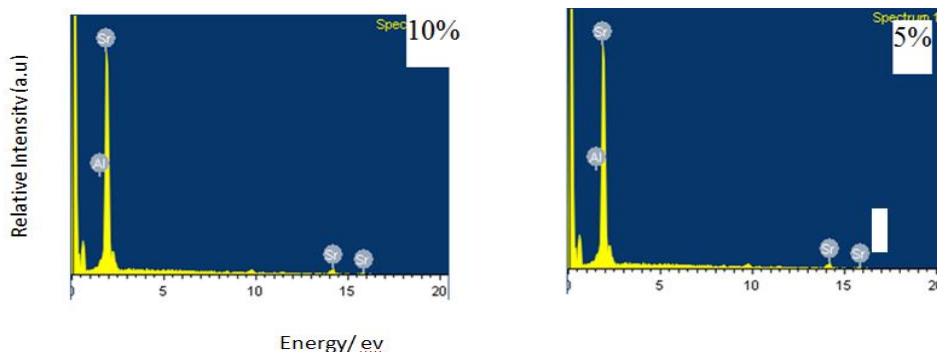


Figure 4: Energy dispersive spectrum of SrAl_4O_7

2. Optical Study

Photoluminescence Analysis

The photoluminescence emission spectra of the SrAl_4O_7 shown in the Figure 5, The PL properties of SrAl_4O_7 nanopowders were measured at room temperature. In this figure, the PL spectra of SrAl_4O_7 consisted of three parts:

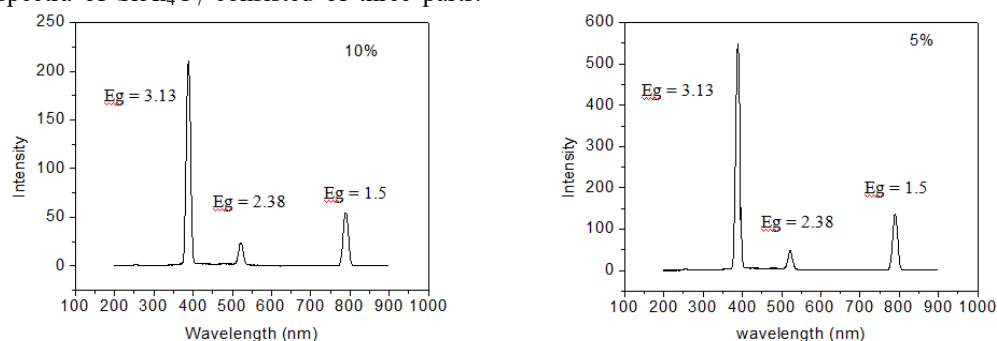


Figure 5: PL spectra of SrAl_4O_7

Five X-ray emission peaks at 0.53, 1.50, 1.82, 2.14, 9.66keV are attributed to the characteristic X-ray emissions of O($K\alpha_1$), Al($K\alpha_1$), Sr($L\alpha_1$), Au($M\alpha_1$) and Au($L\alpha_2$), respectively. The presence of the Au element in the specimen was introduced in the process of Au sputtering for the SEM and elemental analyses.

one weak peak in the blue region, one strong band in bluish green region and other emission bands in red light region. SrAl_4O_7 nanocrystals are found to have increased photoluminescence efficiency.

4. Conclusion

In this paper, by using sol-gel method SrAl_4O_7 nanoparticles for 5 and 10wt% were synthesized. Materials characterization such as; X-ray diffraction (XRD), photoluminescence (PL) emission spectra, scanning electron microscopy (SEM) were analysed. In the results, we report the SrAl_4O_7 phosphor generates a strong emission at 395 nm, 520 nm in green region. The prepared SrAl_4O_7 nanoparticles are applicable for fluorescent lamp and plasma display applications. The prepared Strontium Aluminate nano powder exhibits monoclinic structure.

References

- [1] Chavhan P.M., Anubha Sharma, Kim Koushik, Sol-gel Derived $6\text{CaO} \cdot 6\text{SrO} \cdot 7\text{Al}_2\text{O}_3$ Thin Films using Metal Alkoxides, *Ceram. Int.* 2011; 37: 3413–3417p. Available at: <http://www.sciencedirect.com/science/article/pii/S027288421100530X>
- [2] Chavhan P.M., Govind, Anubha Sharma, *et al.* Structural and Optical Properties of $6\text{CaO} \cdot 6\text{SrO} \cdot 7\text{Al}_2\text{O}_3$ Thin Films Derived by Sol-gel Dip Coating Process, *J. Non-Crystal. Solids* 2011; 357: 1351–1356p. Available at: <http://www.sciencedirect.com/science/article/pii/S0022309310006691>
- [3] Tuomas, Jorma, Jungner, *et al.* Sol-gel Doped Alkaline Earth Aluminates Processed Eu^{2+} - Doped Alkaline Earth Aluminates, *J. Alloy. Compd.* 2002; 341: 76–78p. Available at: <http://www.sciencedirect.com/science/article/pii/S0925838802000683>
- [4] Zuoling, Yaung, Moon, *et al.* Synthesis and Luminescent Properties of Europium-Activated Ca_2SO_4 Phosphors by Sol-gel Method, *J. Lumin.* 2009; 129: 1669–1672p. Available at: <http://www.sciencedirect.com/science/article/pii/S002231309001161>
- [5] T.V.Kolekar, Yadav, Bandgar, *et al.* Synthesis by Sol-gel Method and Characterization of ZnO nanoparticles, *Indian streams Res. J.* 2011; 1: 1–4p. ISSN 2230–7850. Available at: <http://www.isrj.net/UploadedData/36.pdf>

- [6] Hoefsloot A.M., Thijssen P.H.F., Metselaar R., *Silic. Ind.* 1985; 35p. Available at: <http://alexandria.tue.nl/repository/freearticles/620156.pdf>
- [7] Suryanarayana C, Norton MG: *X-ray Diffraction: A Practical Approach*. Plenum Publishing Corporation, New York, 1998. Available at: <http://www.hindawi.com/journals/isrn/2013/369670/ref/>
- [8] Williamson G. K Hall. W. H.: *Acta Met all.*, 1953;1:22p. Available at: http://www.icdd.com/resources/axa/vol40/v40_612.pdf
- [9] Cullity BD. *Elements of X-ray diffraction*, 2nd Edn. New York: Addison Wesley; 1978.
- [10] Dhak D, Pramanik P. *J Am Cer Soc.* 2006; 89: 1014–21p.
- [11] Deng ZX, Wang C, Sun XM, *et al. Inorg Chem.* 2002; 41: 869–73p.
- [12] Nakamoto K. *Infrared Spectra of Inorganic and Coordination Compound*, 4th Edn. Beijing: Chemical Industry Press; 1991.
- [13] Tanabe S, Sugimoto N, Ito S, Hanada T, *J Luminesc.* 87, (2000) 670-672.
- [14] DeLoach LD, Payne SA, Chase LL, Smith LK, Kway WL, Krupke WF, *IEEE J Quantum Electron*, 29, (1993) 1179-1191.
- [15] Soukka T, Kuningas K, Rantanen T, Haaslahti V, Lovgren T, *J Fluoresc*, 15, (2005) 513-528.
- [16] Das GK, Yang-Tan TT, *J Phys Chem C*, 112, (2008) 11211-11217.
- [17] Xiao Q, Si Z, Yu Z, Qiu G, *Mater Sci Eng B*, 137, (2007) 189-194.
- [18] H.Ryu, K.S Bartwal *Journal of Alloys and Compounds* 574, (2013) 331-334.